Heliyon 10 (2024) e32790

Contents lists available at ScienceDirect

Heliyon

journal homepage: www.cell.com/heliyon

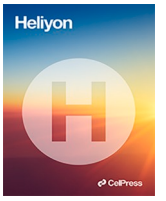

Research article

The metabolomics analysis of cecal contents elucidates significant metabolites involved in the therapeutic effects of total flavonoids derived from Sonchus arvensis L. in male C57BL/6 mice with ulcerative colitis

Naidan Chang [a,1], Wei wei [c,1], Shihe Wang [a], Shenghua Hou [a], Yilei Sui [a], Taoyang [a], Jing He [a], Yachao Ren [a,d,**], Guoyou Chen [a,*], Chunlei Bu [a,b,***]

[a] Harbin Medical University 163319, China
[b] Fifth Affiliated Hospital, Harbin Medical University, Daqing, 163319, China
[c] Daqing Oilfield Genaral Hospital, Daqing, 163319, China
[d] School of Chemistry and Chemical Engineering, Tianjin University of Technology, Tianjin, 300000, China

ARTICLE INFO

Keywords:
Ulcerative colitis
Total flavonoids of sonchus arvensis L.
Key metabolites
Metabonomics
Cecal contents of male C57BL/6 mice

ABSTRACT

Ulcerative colitis (UC), an inflammatory disease affecting the colon and rectal mucosa, is characterized by chronic and heterogeneous behavior of unknown origin. The primary cause of UC is chronic inflammation, which is closely linked to the development of colorectal cancer. Sonchus arvensis L. (SAL), a plant consumed worldwide for its nutritional and medicinal properties, holds significance in this context. In this study, we employed the total flavone in SAL as a treatment for male C57BL/6 mice with UC. The cecal contents metabolic profile of C57BL/6 mice in different groups, including UC (group ML; n = 5), UC treated with aspirin (group AN; n = 5), UC treated with the total flavone in SAL (group FE; n = 5), and healthy male C57BL/6 mice (group CL; n = 5), was examined using UHPLC-Triple-TOF-MS. Through the identification of variations in key metabolites associated with UC and the exploration of their underlying biological mechanisms, our understanding of the pathological processes underlying this condition has been enhanced.

This study identified a total of seventy-three metabolites that have a significant impact on UC. Notably, the composition of total flavone in SAL, a medication used for UC treatment, differs from that of aspirin due to the presence of four distinct metabolites (13,14-Dihydro-15-keto-PGE2, Prostaglandin I2 (PGI2), (20R,22R)-20,22-dihydroxycholesterol, and PS (18:1(9Z)/0:0)). These metabolites possess unique characteristics that set them apart. Moreover, the study identified a total of eleven pathways that were significantly enriched in mice with UC, including Aminoacyl-tRNA biosynthesis, Valine, leucine and isoleucine biosynthesis, Linoleic acid metabolism, PPAR signaling pathway, mTOR signaling pathway, Valine, leucine and isoleucine degradation, Lysine degradation, VEGF signaling pathway, Melanogenesis, Endocrine and other factor-regulated

* Corresponding author.
** Corresponding author. School of Chemistry and Chemical Engineering, Tianjin University of Technology, tianjin, 300000, China, Harbin Medical University, 163319, China.
*** Corresponding author. Fifth Affiliated Hospital, Harbin Medical University, Daqing, 163319, China, Harbin Medical University, 163319, China.
E-mail addresses: yachaoren@163.com (Y. Ren), 46555799@qq.com (G. Chen), Bcl588@126.com (C. Bu).
[1] These authors have contributed equally to this work and share first authorship.

https://doi.org/10.1016/j.heliyon.2024.e32790
Received 1 January 2024; Received in revised form 9 June 2024; Accepted 10 June 2024
Available online 16 June 2024

calcium reabsorption, and Cocaine addiction. These findings contribute to a better understanding of the metabolic variations in UC following total flavonoids of SAL therapy and provide valuable insights for the treatment of UC.Keywords: Ulcerative colitis; Total flavonoids of Sonchus arvensis L.; Key metabolites; Metabonomics; Cecal contents of male C57BL/6 mice.

1. Introduction

Ulcerative colitis (UC) is a chronic and idiopathic colitis, lacking a definitive etiology [1–3]. The global prevalence of UC has been observed to increase in recent years [4,5]. Therefore, the provision of efficacious therapeutic interventions for UC is of paramount importance in mitigating the potential complications associated with this condition. Inflammatory responses represent a prevalent manifestation of UC [6,7]. Moreover, a strong correlation has been established between UC and the development of colitis-associated cancer (CAC) [8,9].

There are reports describing the important effect of diet on UC [10]. A positive correlation exists between Anti-Saccharomyces cerevisiae (ASCA) and UC occurrence, possibly related to antigen antibody responses [11]. Sonchus arvensis L., a plant from Chinese folklore, is commonly employed in dietary and traditional medicine for the treatment of inflammatory ailments [12]. Presently, scientific investigations have revealed that extracts derived from Sonchus arvensis L. possess noteworthy antioxidant, antibacterial, antitumor, and anti-inflammatory attributes [13–16].

In this study, the anti-inflammatory effects of SAL extract were assessed in male C57BL/6 mice UC models. The decision to employ total flavonoids from SAL extract was based on a multitude of studies that have consistently highlighted their anti-inflammatory, anti-carcinogenic, and cytoprotective attributes, thereby establishing them as the dominant subgroup within the polyphenol classification [17,18]. Nevertheless, the precise mechanism by which its metabolites contribute to the anti-inflammatory action remains undisclosed.

Metabolomics has emerged as a significant discipline within the field of biology [19,20]. It serves as a valuable technique for the identification and characterization of small organic metabolites in biological systems [21]. The integration of ultra-performance liquid chromatography with electrospray ionization quadrupole time-of-flight mass spectrometry (UHPLC-ESI-Q-TOF-MS) is a crucial component in the application of metabolomics [22]. Consequently, metabolomic analysis enables the identification of physiological and pathological metabolite mechanisms involved in the progression of diseases.

In this study, male C57BL/6 mice with UC were treated with either a classical drug (aspirin) or the total flavonoids of traditional herb medicine (SAL extract). The cecal contents metabolic profile of the C57BL/6 mice in the UC group (group ML; n = 5 C57BL/6 mice with UC), the positive control group (group AN; n = 5 C57BL/6 mice treated with aspirin), the treatment group (group FE; n = 5 C57BL/6 mice treated with the total flavonoids of SAL extract), and the healthy control group (group CL; n = 5 healthy male C57BL/6 mice) was investigated using UHPLC-ESI-Q-TOF-MS. In the treatment group of male C57BL/6 mice with UC, a significant correlation was observed between 73 metabolites and various substances, including arachidonic acids (Fig. 6), amino acids (Fig. 7), fatty acids (Fig. 8), and others (Fig. 9) such as 5(S)-HETrE, 8(S)-HETrE, 8-iso-PGE2, Indole-3-carbinol, 9(S)-HODE, 14(Z)-Eicosenoic Acid, 11(S)-HEDE, C18_Sphingosine, and Homoveratric acid.

The extraction of flavonoids from SAL for the treatment of UC results in the production of four metabolites that exhibit distinct and noteworthy characteristics, which differ from those of aspirin. With the exception of 13,14-Dihydro-15-keto-PGE2 (Fig. 6), the metabolites of Prostaglandin I2 (PGI2) (Fig. 6), (20R,22R)-20,22-dihydroxycholesterol (Fig. 9A), and PS(18:1(9Z)/0:0) (Fig. 9A) indicate that FE will induce milder effects compared to AN.

During the course of this study, metabolomic analyses have identified several metabolites that play a regulatory role in various pathways, including Aminoacyl-tRNA biosynthesis, Valine, leucine and isoleucine biosynthesis, Linoleic acid metabolism, PPAR signaling pathway, mTOR signaling pathway, Valine, leucine and isoleucine degradation, Lysine degradation, VEGF signaling pathway, Melanogenesis, Endocrine and other factor-regulated calcium reabsorption, and Cocaine addiction. These findings suggest that these metabolites could serve as potential therapeutic targets for male C57BL/6 mice with UC.

2. Materials and methods

2.1. Animals

The Male C57BL/6 mice (21–23g) were obtained from Charles River Laboratories (Beijing, China) and were housed under SPF conditions. All experimental protocols for all animal experiments were approved by the ethics committee of Daqing Campus of Harbin Medical University (LLDQXQ2022031).

2.2. Preparation of total flavone extract

One hundred grams of the entire SAL plant were fragmented and subsequently dissolved in a 50 % ethanol solution. The resulting mixture was subjected to ultrasonication for a duration of 0.5 h, repeated three times. Following extraction with petroleum ether, the ethanol solution was gathered and concentrated using a rotary evaporator. Subsequently, the concentrated extracts were desiccated in a freezer (Scientz-100FG/A) and stored at a temperature of −20 °C.

2.3. Establishment of colitis model and treatment

In this study, a mouse model of chronic acute colitis was created through administration of 0.2 ml of 0.6 g/ml dextran sodium sulfate (DSS) on a daily basis for a duration of 7 days. DSS was supplied by MP Biomedicals (Irvine, CA, USA). Following this period, the mice was subjected to pentabarbital anesthesia to observe the changes in inflammation. The efficacy of the validation model utilized in this research was confirmed, as depicted in Fig. 10.

Among the animals, four groups were selected in a random manner for the purpose of this study: the control plus saline group (referred to as CL), the DSS plus saline group (referred to as ML), the aspirin group (0.1 g/kg) plus DSS as positive controls (referred to as AN), and the treatment group receiving total flavone from Sonchus arvensis L (0.85 g/kg) plus DSS (referred to as FE). As depicted in Fig. 1, all the animals were categorized based on their experimental timeline. To assess the preventive effect of FE on DSS-induced acute colitis in the experimental animals, FE was administered daily via gavage for a duration of twenty-one days. In the CL and ML groups, normal saline solutions were administered on a daily basis. As a positive control, the effect of Aspirins was further validated by treating C57BL/6 mice daily after DSS treatment for seven days.

The model of DSS-induced acute colitis began on day 14 and ended on Day 21. The anti-inflammatory treatment involving aspirin spans a duration of 7 days, and FE started on day 1, prophylaxis for 14 days and treatment for 7 days.

CL, control group, n = 5; ML, dextran sodium sulfate group, n = 5; AN, aspirin treatment group, n = 5; FE, total flavone from Sonchus arvensis L treatment group, n = 5.

2.4. Non-targeted metabonomic analysis

An ultra-high-pressure liquid chromatography system (Agilent 1290, USA) was used for the chromatography. In this experiment, the chromatographic column was ACQUITY UHPLC HSS T3 (1.8 μm; 2.1 × 100 mm) (Waters). Formic acid was included in mobile phases A and B at a concentration of 0.1 % in water and 0.1 % in acetonitrile, respectively [23]. Elution was performed in the following manner: 5 % B for 1 min, followed by 10 % B within 1 min, followed by 95 % B within 12 min, then held for 2 min. Within 1 min, it was changed linearly to 5 % B and held for 3 min. A temperature of 35 °C was used for the analytical column and a temperature of 4 °C was used for the autosampler. Each run consisted of 5 μL of sample, and the column eluent was analysed directly on the MS [23].The cecal contents (0.2g) was mixed with 4 vol of methanol/acetonitrile (1:1, v/v) for analysis. After shaking for 30 s, all samples were ultrasonically treated for 10 min in an ice-cold water bath. A 2-h incubation at −20 °C was followed by 15 min at 4 °C centrifugation with 13,000×*g* to facilitate protein precipitation. A supernatant of cecal contents was collected, dried under vacuum, and centrifuged at 4 °C. Following resuspension in 200 μL of methanol/acetonitrile (1:1), shaking for 30 s, and centrifugation at 13,000×*g* for 15 min at 4 °C, the aliquots were dried. The supernatant was analysed on a UHPLC system with a Q-TOF system (Agilent 6545, USA) using approximately 150 μL. A quality control (QC) test was performed after each analysis of five samples.

Data were obtained using the auto MS/MS mode from 50 to 1100 *m/z*. Collision energies for collision-induced dissociation were 20 V and 40 V. MS parameters were set as follows: ion source dry gas temperature, 320 °C; N_2 gas flow, 8L/min; sheath gas temperature, 350 °C; sheath gas flow, 12 L/min; ion spray voltage, 4000 V (positive ion) and 3500 V (negative ion).

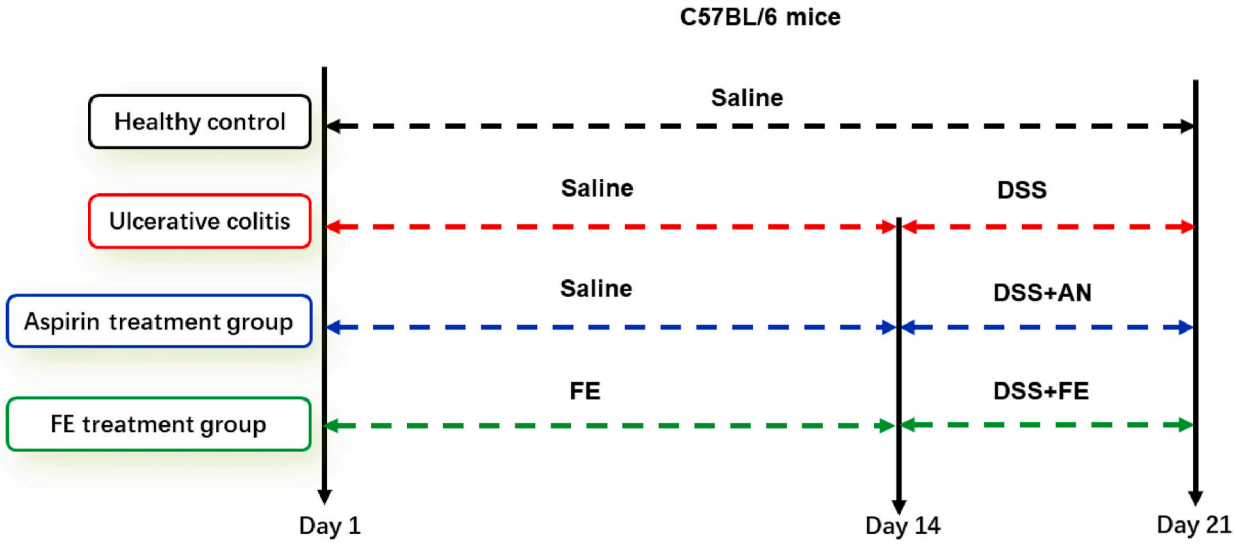

Fig. 1. Illustrates the establishment of a colitis model and its subsequent treatment.

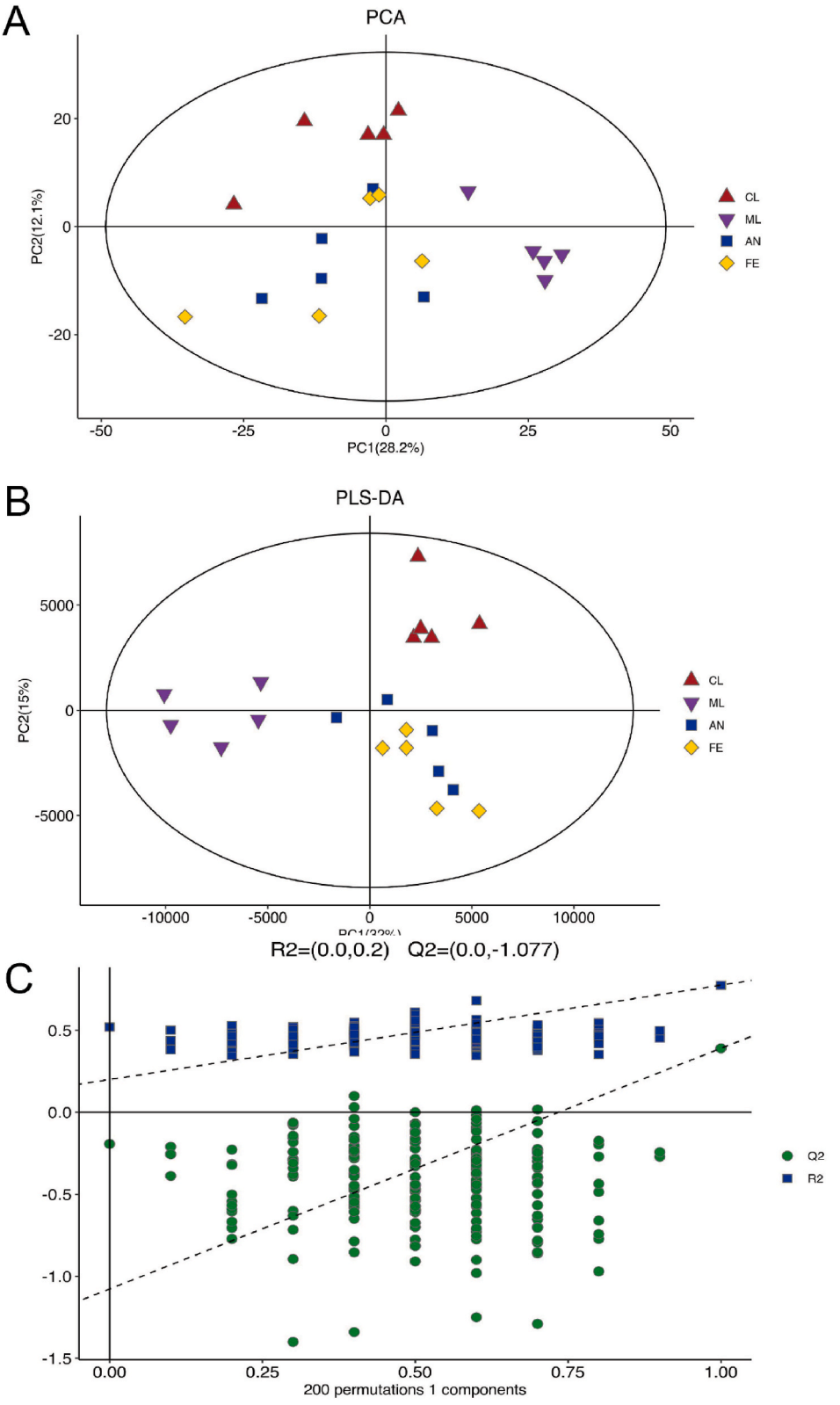

Fig. 2. Metabolomic analysis the effects of drug treatment on ulcerative colitis (UC) using UHPLC-TOF-MS. (A) PCA; (B) PLS-DA; (C) Permutation tests.

2.5. Data collection and analysis

The Analysis Base File Converter was used to convert data files from the Q-TOF-MS system to.abf format. The following parameters were used for peak detection, chromatogram deconvolution, and other data analyses: alignment-MS1 tolerance, 0.01 Da; retention time tolerance, 0.2 min; identification accurate mass tolerance (MS1), 0.005 Da; MS2, 0.05Da; identification score cut off, 60 %. Metabolites and metabolic pathways were identified using HMDB (http://www.hmdb.ca/), METLIN (http://metlin.scripps.edu/), Massbank (http://www.massbank.jp) and KEGG (http://www.kegg.com/) databases. In order to enhance precision, the identified metabolites were cross-validated utilizing a laboratory standard library.

SIMCA-P software (version 14.1, Umetrics, Umea, Sweden) was used for the multivariate statistical analysis. A principal component analysis (PCA) was performed on the matrix imported into R to observe the overall distribution of samples and assess the stability of the whole process. Metabolites were distinguished between groups using partial least squares discriminant analysis (PLS-DA). Seven-fold cross-validation and 200 permutation tests (response permutation testing [RPT]) were performed to evaluate the model's quality. A permutation test was used to assess the validity of the model and its degree of overfitting. A VIP >1.0 and a p-value of 0.05 indicate that there is a significant difference. A p-value of 00.05 indicates that there is a significant difference between two groups compared using the Mann–Whitney *U* test. For multiple groups, the false discovery rate (FDR) was applied ($p < 0.10$).

3. Results

3.1. Metabolomic analysis of the drug treatment of UC via UHPLC-TOF-MS

In order to ascertain the essential metabolites linked to the treatment of UC, the metabolic profiles of the cecal contents of male

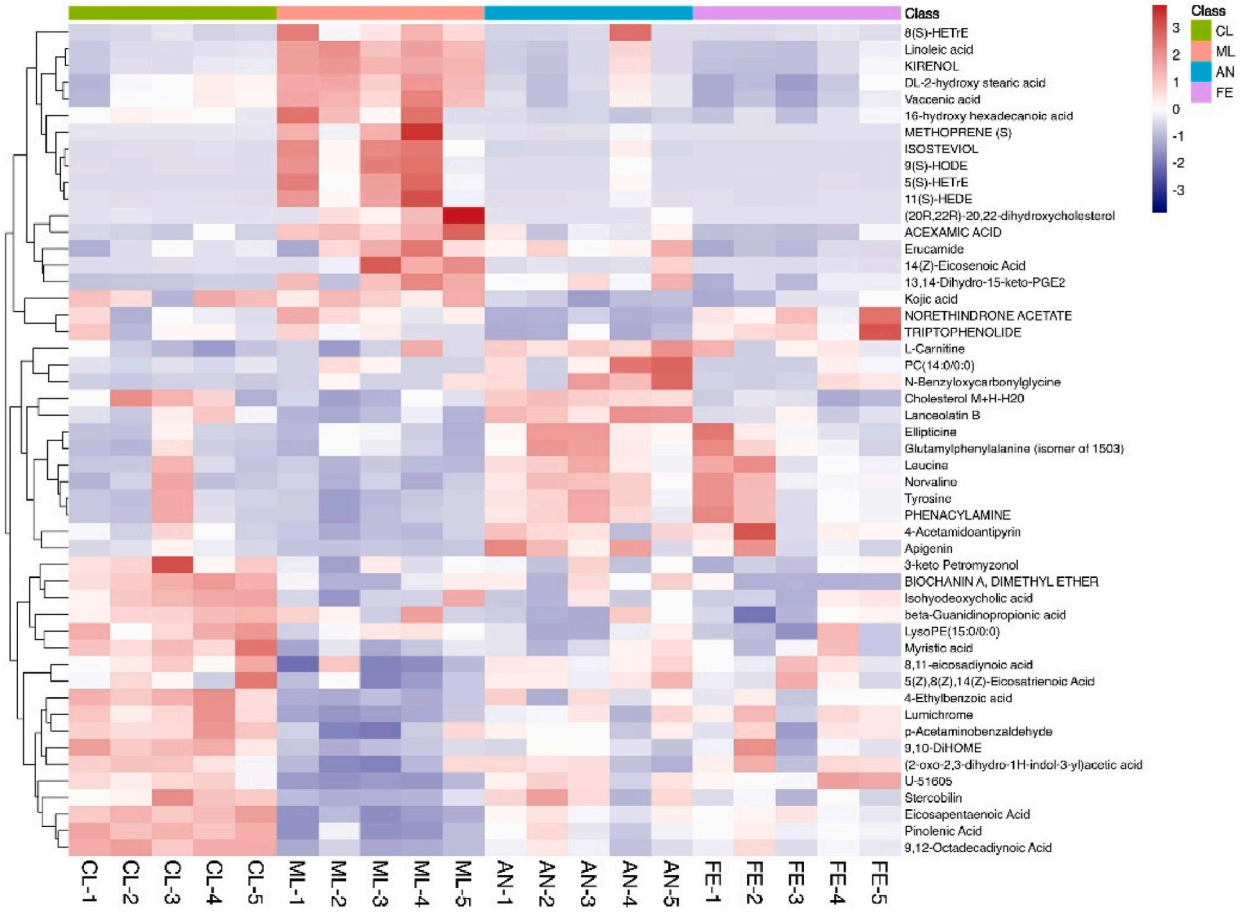

Fig. 3. Heat maps of metabolites The abscissa indicates the sample name, and the ordinate indicates the differential metabolites. The color gradient from blue to red represents the abundance of metabolites' expression, ranging from low to high. In other words, the more red the color, the higher the expression abundance of differential metabolites. CL, control group, n = 5; ML, dextran sodium sulfate group, n = 5; AN, aspirin treatment group, n = 5; FE, total flavone from Sonchus arvensis L treatment group, n = 5. (For interpretation of the references to color in this figure legend, the reader is referred to the Web version of this article.)

C57BL/6 mice in four distinct groups (CL, ML, AN, and FE groups) were subjected to analysis using UHPLC-TOF-MS. The multivariate statistical analysis would involve the application of unsupervised principal component analysis (PCA) to investigate the overall distribution among the samples and evaluate the reliability of the entire analysis procedure. Following this, supervised partial least squares analysis (PLS-DA) was utilized to ascertain the overall discrepancies in metabolic profiles between the groups and identify the unique metabolites that distinguish the groups. The data were analysed using the SIMCA-P software, and the results of PCA and PLS-DA can be observed in Fig. 2A and B. Metabolite differences were examined among the CL, ML, AN, and FE groups. The model's reliability

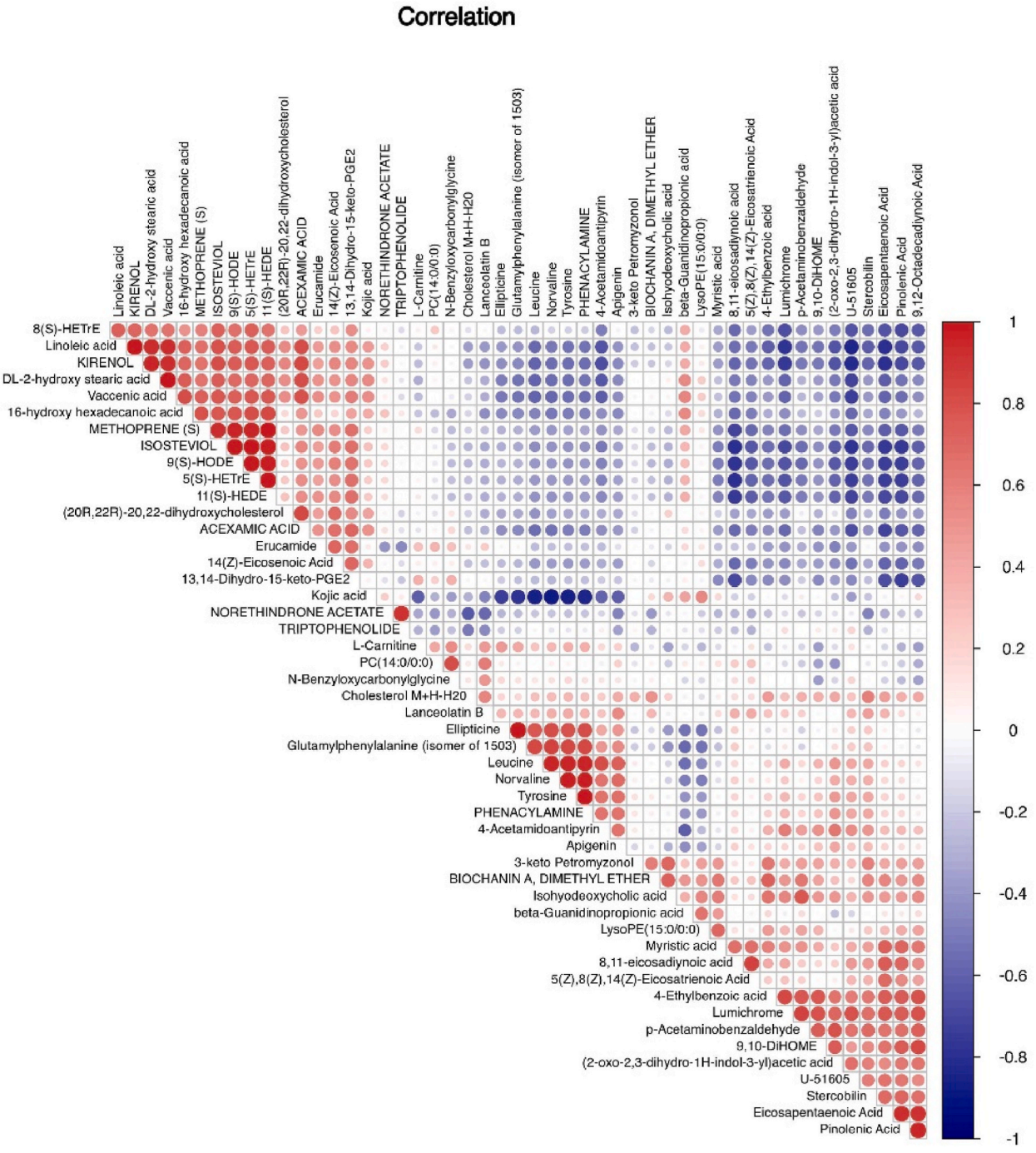

Fig. 4. Pearson correlation analysis Red color indicates a positive correlation, while blue color indicates a negative correlation. A larger dot indicates a higher correlation coefficient between the two variables. (For interpretation of the references to color in this figure legend, the reader is referred to the Web version of this article.)

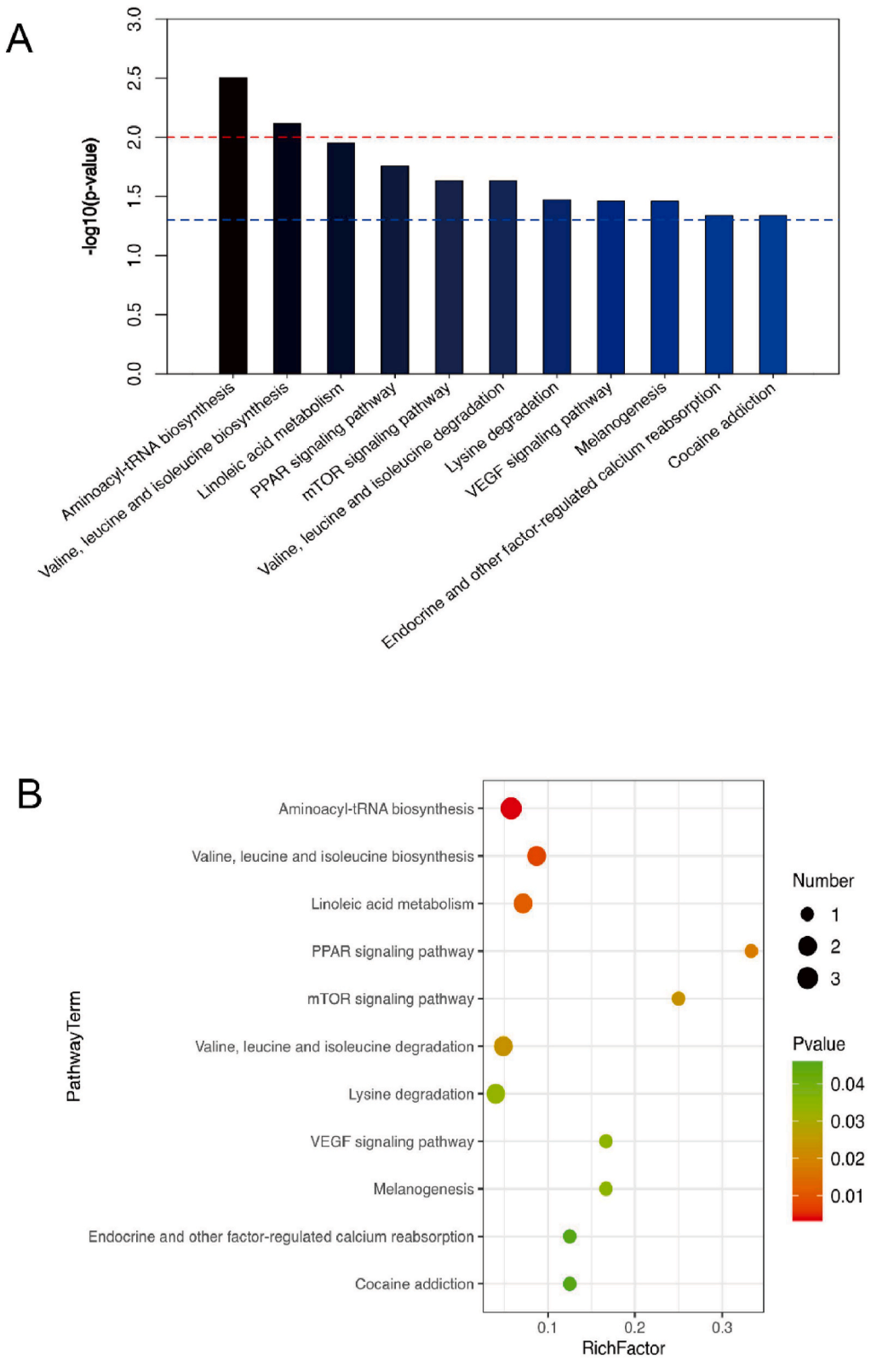

(caption on next page)

Fig. 5. Pathways enrichment analysis (A) The abscissa represents the -log10 p value of each pathway, while the ordinate represents the names of the different pathways. The red line indicates a p-value of 0.01, the blue line indicates a p-value of 0.05, and when the top of the column is higher than the blue line, the signal pathway represented is significant. (B) The x-axis represents the rich factor, which was determined by dividing the count of differentially expressed metabolites in the relevant metabolic pathway by the total number of identified metabolites in that pathway. A higher rich factor indicates a greater level of pathway enrichment. The color gradient on the scale ranges from green to red, with p-values gradually decreasing. Additionally, the size of the bubble corresponds to the number of metabolites present in the pathway. (For interpretation of the references to color in this figure legend, the reader is referred to the Web version of this article.)

was confirmed as permutation tests did not indicate overfitting, as depicted in Fig. 2C. Supplemental Table 1 presents the identification of various crucial metabolites and metabolic pathways linked to treatment within the cecal contents of male C57BL/6 mice.

3.2. Visualisation of differentially expressed metabolites using heat maps

As shown in Fig. 3, from 8(S)-HETrE to kojic acid, a significant increase in the MS group and a decrease expression were observed following with AN or FE treatment. Second, we explored that some metabolites were the decreased expression from 3-keto petromyzonol to 9,12-octadecadiynoic acid in the MS group. Third, from 3-keto petromyzonol to 9,12-octadecadiynoic acid, some target metabolites were elevated after AN or FE treatment.

3.3. Metabolite–metabolite correlation analysis

Pearson correlation analysis was conducted to investigate the relationship between the identified metabolites in male C57BL/6 mice with UC. The results, depicted in Fig. 4, demonstrate the correlation among the top 50 differentially expressed metabolites. Although the functional properties of 8(S)-HETrE, a monohydroxy polyunsaturated fatty acid, have not been extensively characterized, it is anticipated to exhibit similar behavior to 8(S)-HETE. Notably, 8(S)-HETrE exhibited a significant positive correlation with linoleic acid, kirenol, DL-2-hydroxy stearic acid, vaccenic acid, methoprene (s), isosteviol, 5(S)-HETrE, 9(S)-HODE, and 11(S)-HEDE. In contrast, 8(S)-HETrE exhibited a noteworthy inverse association with 4-acetamidoantipyrin, 8,11-eicosadiynoic acid, 4-ethylbenzoic acid, lumichrome, U-51605, stercobilin, eicosapentaenoic acid, pinolenic acid, and 9,12-octadecadiynoic acid.

3.4. KEGG pathway enrichment analysis

In Fig. 5, significant enrichment of 11 pathways was observed in the four groups, which included Aminoacyl-tRNA biosynthesis, Valine, leucine and isoleucine biosynthesis, Linoleic acid metabolism, PPAR signaling pathway, mTOR signaling pathway, Valine, leucine and isoleucine degradation, Lysine degradation, VEGF signaling pathway, Melanogenesis, Endocrine and other factor-regulated calcium reabsorption, and Cocaine addiction. The results depicted in Fig. 5A and B demonstrate that aminoacyl-tRNA biosynthesis was the pathway that exhibited the most significant enrichment among the four groups.

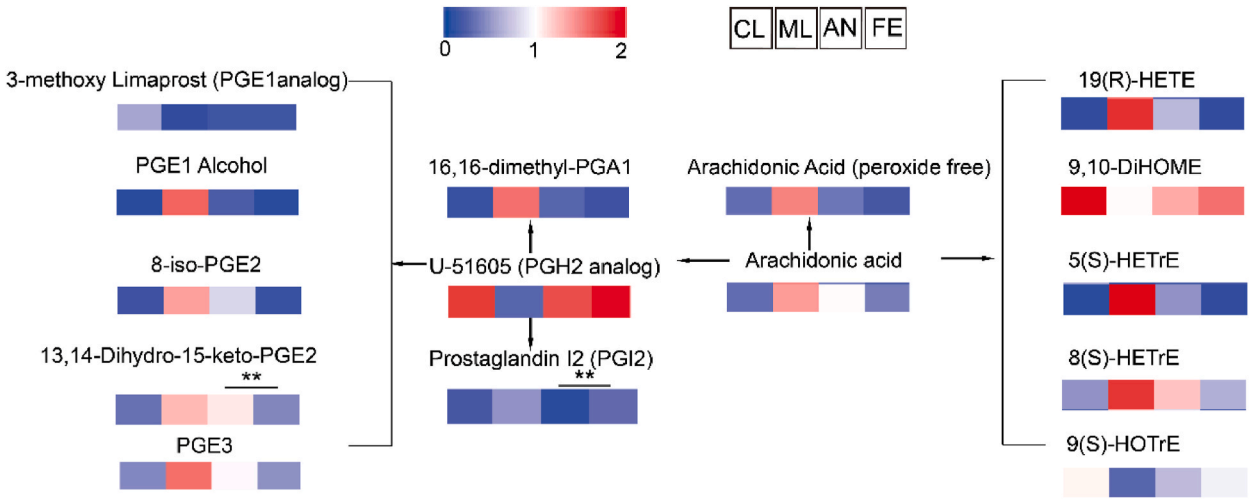

Fig. 6. Metabolites of arachidonic acid The red color signifies an elevated content in comparison to the normal group, while the corresponding blue color signifies a reduced content relative to the normal group. CL, control group, n = 5; ML, dextran sodium sulfate group, n = 5; AN, aspirin treatment group, n = 5; FE, total flavone from Sonchus arvensis L treatment group, n = 5. (For interpretation of the references to color in this figure legend, the reader is referred to the Web version of this article.)

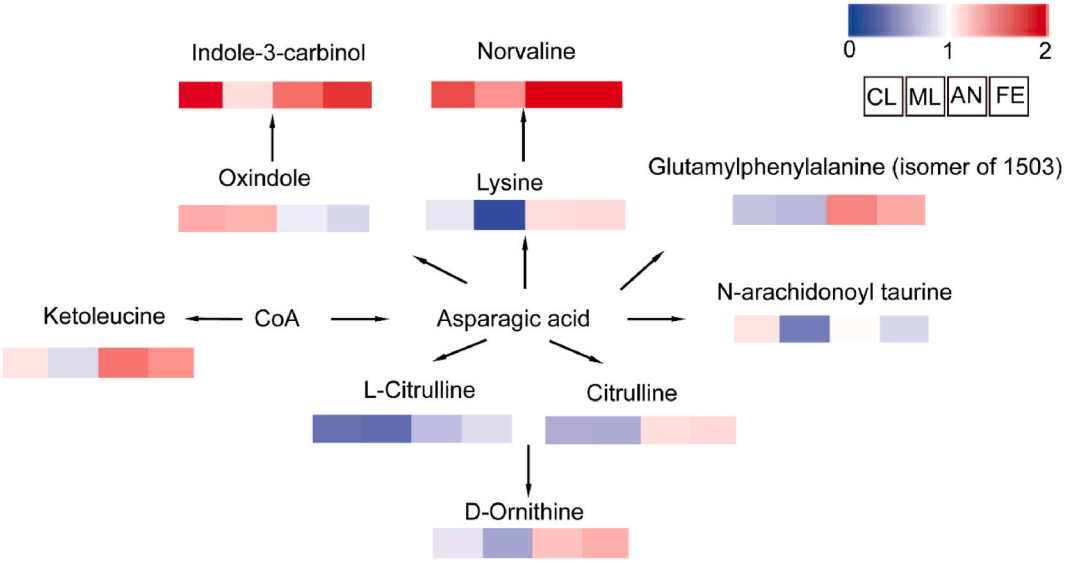

Fig. 7. Amino acids.

3.5. *Metabolites of arachidonic acid*

In this study, the modulation of inflammation was observed through the examination of specific metabolites of arachidonic acid [22]. The eleven metabolites investigated were 5(S)-HETrE, 8(S)-HETrE, 8-iso-PGE2, 13,14-Dihydro-15-keto-PGE2, 16,16-dimethyl-PGA1, 19(R)-HETE, Arachidonic Acid (peroxide free), Arachidonic_acid, PGE1 Alcohol, Prostaglandin I2 (PGI2), and PGE3. Notably, these metabolites exhibited a significant increase in the ML group, but their levels decreased following medication in the AN and FE groups.

In Fig. 6, it was observed that four metabolites of arachidonic acid, namely U-51605 (PGH2 analog), 3-methoxy Limaprost (PGE1 analog), 9(S)-HOTrE, and 9,10-DiHOME, exhibited significant decreases between the CL and ML groups. Following treatment with aspirin or total flavonoids, these metabolites were found to be upregulated, with the exception of 3-methoxy Limaprost (PGE1 analog). Notably, the disparities in the effects of the two drugs during UC treatment were of particular interest. The total flavone from Sonchus

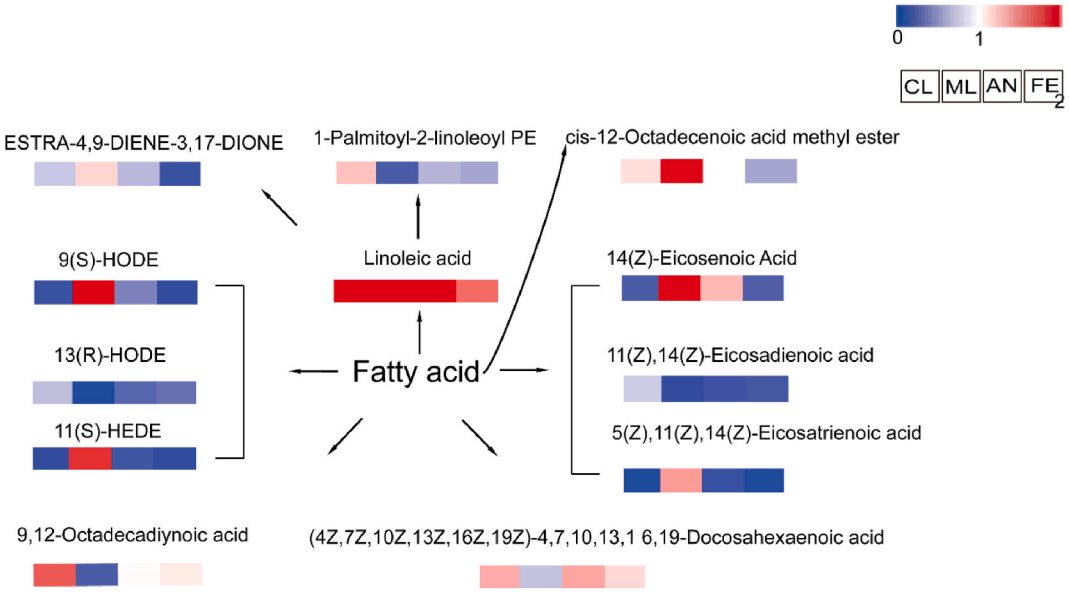

Fig. 8. Fatty acids. The red color signifies an elevated content in comparison to the normal group, while the corresponding blue color signifies a reduced content relative to the normal group. CL, control group, n = 5; ML, dextran sodium sulfate group, n = 5; AN, aspirin treatment group, n = 5; FE, total flavone from Sonchus arvensis L treatment group, n = 5. (For interpretation of the references to color in this figure legend, the reader is referred to the Web version of this article.)

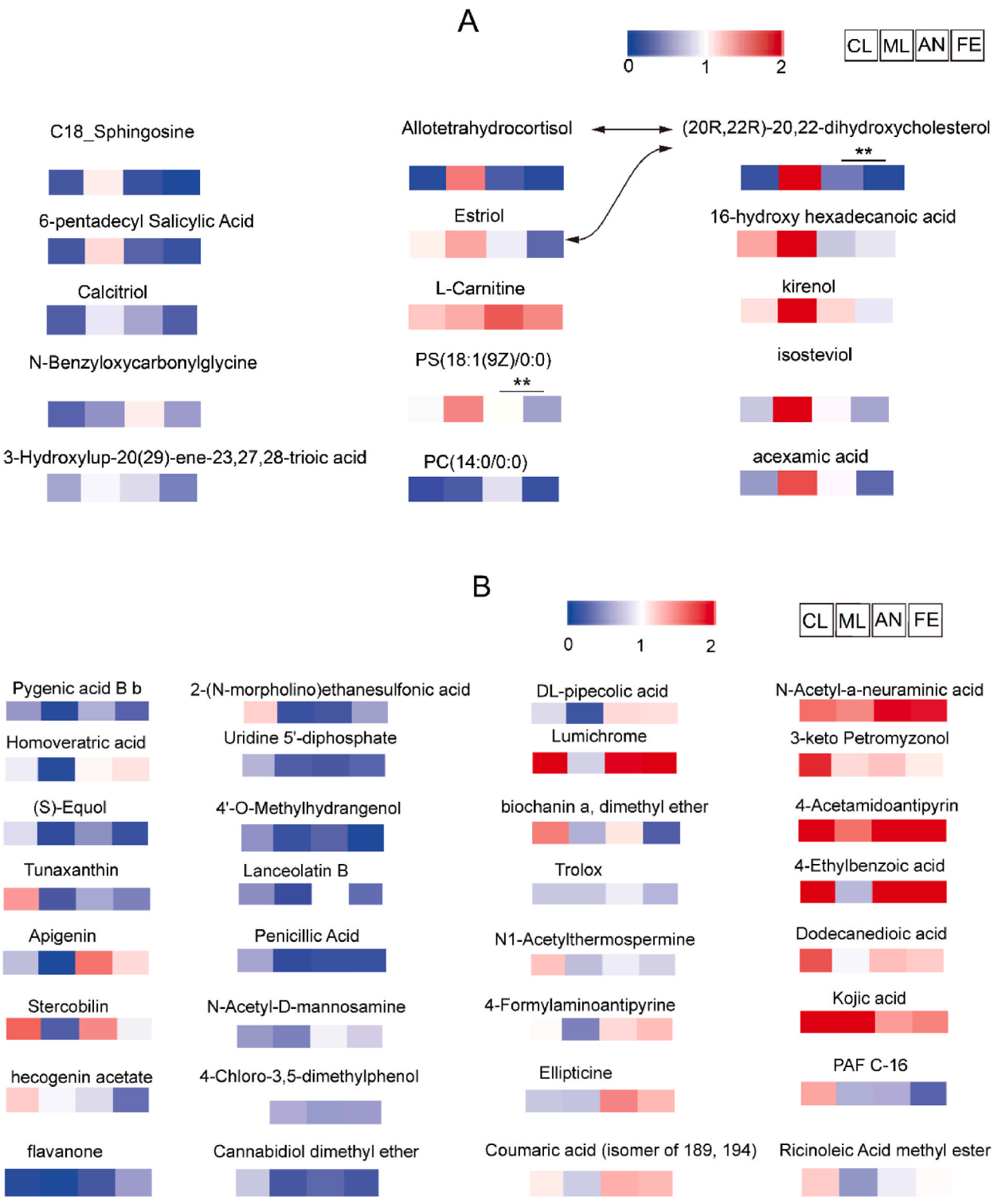

Fig. 9. Others metabolites. (A) Upregulated metabolites (B) downregulated metabolites. The red color signifies an elevated content in comparison to the normal group, while the corresponding blue color signifies a reduced content relative to the normal group. CL, control group; ML, dextran sodium sulfate group; AN, aspirin treatment group; FE, total flavone from Sonchus arvensis L treatment group. (For interpretation of the references to color in this figure legend, the reader is referred to the Web version of this article.)

arvensis L demonstrated greater efficacy than aspirin in terms of 13,14-Dihydro-15-keto-PGE2, while the opposite trend was observed in the metabolite of PGI2.

3.6. Amino acids

The red color signifies an elevated content in comparison to the normal group, while the corresponding blue color signifies a reduced content relative to the normal group. CL, control group, n = 5; ML, dextran sodium sulfate group, n = 5; AN, aspirin treatment group, n = 5; FE, total flavone from Sonchus arvensis L treatment group, n = 5.

Fig. 7 demonstrates that the ML group exhibited decreased expression of 10 amino acids-related metabolites compared to the CL group. Moreover, significant alterations in these metabolites were observed in the AN and FE groups. The findings from Fig. 7 suggest that the drug potentially exerts its effects by modulating the aforementioned 10 amino acids-related metabolites, which play a crucial role in the regulation of UC in male C57BL/6 mice.

3.7. Fatty acids

Metabolites of Fatty acid that exhibited differential expression were identified as a means to distinguish among male C57BL/6 mice within the four groups. Fig. 8 demonstrates that 11 metabolites may be implicated in the pathogenesis of UC. Specifically, the expression levels of Estra-4,9-diene-3,17-dione, *cis*-12-Octadecenoic Acid methyl ester, 9(S)-HODE, 14(Z)-Eicosenoic Acid, 11(S)-HEDE, Methoprene(s), and 5(Z),11(Z),14(Z)-Eicosatrienoic acid were observed to increase, while the expression levels of 13(R)-HODE, 1-Palmitoyl-2-linoleoyl PE, 9,12-Octadecadiynoic Acid, and (4Z,7Z,10Z,13Z,16Z,19Z)-4,7,10,13,16,19-Docosahexaenoic acid were observed to decrease in the UC group. However, these alterations were found to be reversed following treatment with aspirin or total flavonoids extracted by SAL.

3.8. Others metabolites

The findings of the metabolite analysis are presented in Fig. 9, which displays the results for various metabolites. Within the UC group (ML), it was observed that 15 metabolites were upregulated (Fig. 9A), while 32 metabolites were downregulated (Fig. 9B). Notably, the administration of aspirin or total flavonoids extracted from SAL resulted in a reversal of most of these changes. Interestingly, the two drugs exhibited distinct effects during the treatment. Specifically, the total flavone from Sonchus arvensis L showed greater efficacy in (20R,22R)-20,22-dihydroxycholesterol, whereas the opposite trend was observed for the metabolite PS(18:1(9Z)/0:0).

3.9. HE staining results

Based on the findings presented in Fig. 2C, histopathological examination (HE analysis) was employed to assess the extent of colonic inflammation. In the ML group, there was evident degeneration and necrosis of mucosal epithelial cells, significant reduction in intestinal glands, degeneration and necrosis of glandular epithelium, as well as loose and inflamed interstitial edema. However, when a total flavone extract from SAL or aspirin was administered to mice with DSS-induced UC, notable improvements in the pathological alterations were observed (Fig. 10).

4. Discussion

Ulcerative colitis (UC) is a prevalent chronic gastrointestinal disorder. Nevertheless, the precise metabolic mechanisms responsible for the pathogenesis of UC are yet to be fully elucidated. The identification of pivotal metabolites holds the potential to shed light on these underlying mechanisms and facilitate the development of strategies for timely diagnosis, a crucial aspect for the effective

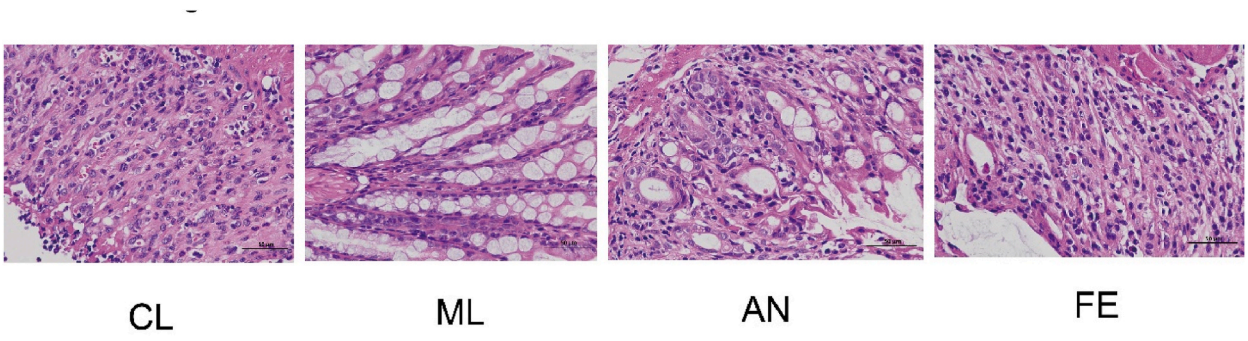

Fig. 10. A histological evaluation of the colons of each experimental group was conducted (H&E staining × 400). CL, healthy C57BL/6 mice, n = 5; ML, mice with UC, n = 5; AN, mice treated with aspirin, n = 5; FE, mice treated with the total flavonoids extracted by Sonchus arvensis L., n = 5.

management of UC. In this investigation, we successfully identified significant metabolites and pathways associated with the treatment of UC through the utilization of ultra-high-performance liquid chromatography-tandem mass spectrometry (UHPLC-MS-MS) to extract total flavonoids from SAL.

4.1. Key metabolites

Metabolites of arachidonic acids (Fig. 6), amino acids (Fig. 7), Fatty acids (Fig. 8) and others compounds (Fig. 9), including 5(S)-HETrE, 8(S)-HETrE, 8-iso-PGE2, Indole-3-carbinol, 9(S)-HODE, 14(Z)-Eicosenoic Acid, 11(S)-HEDE, C18_Sphingosine, and Homoveratric acid, have the potential to exert a notable influence on ulcerative colitis in male C57BL/6 mice.

During the course of this study, the analysis of metabolomics in cecal contents provided clear evidence that the development of the disease was influenced by derivatives of arachidonic acid. Specifically, there were seven metabolites in the arachidonic acid pathways that were upregulated, while four metabolites were downregulated. Additionally, the involvement of x-HETrEs, a polyunsaturated fatty acid (as depicted in Fig. 6), was observed in both tumorigenesis and the metabolism of arachidonic acid, as previously reported [24].

The x-HETEs, which are LOX metabolites of arachidonic acid (Fig. 6), exhibit diverse impacts on the vasculature, oxidative stress, infectious diseases, and tumor inhibition [25–28].Within a healthy endothelium, platelet adhesion and activation are inhibited by prostacyclin (PGI2) and nitric oxide. However, under pathological conditions, excessive adhesion of platelets and leukocytes leads to inflammation and tissue damage [29]. The findings of PGI2 (Fig. 6) derived from this investigation further validate the aforementioned observation. Therefore, it would be beneficial to undertake metabolomics investigations that encompass the entirety of the arachidonic acid metabolic pathway, as well as interconnected pathways of fatty acid metabolism, to enhance comprehension of their collective involvement in the regulation of UC.

Previous studies had demonstrated the involvement of the Notch-AhR-IL-22 axis in chronic viral infections [30,31]. Indole-3-carbinol, depicted in Fig. 7, had been shown to activate AhR [32]. Insufficient AhR ligands or AhR deficiency in the intestine led to heightened immune activation and inflammation in the intestinal tract [32]. There was evidence suggesting that indole-3-carbinol possessed the ability to inhibit melanoma cell proliferation [33]. Furthermore, as dietary plant micronutrients, indole-3-carbinol exhibited inhibitory effects on carcinogenesis.

The present study demonstrates that the extraction of flavonoids from SAL and aspirin effectively ameliorated cecal inflammation by regulating indole-3-carbinol, as evidenced by metabolomics analysis (Fig. 7). Furthermore, the assessment of enterocyte function biomarkers revealed a significant increase in L-Citrulline levels (Fig. 7) [34]. Conversely, the incomplete breakdown of branched-chain amino acids led to the accumulation of ketoleucine (Fig. 7), an aberrant metabolite [35]. In summary, the observed reduction in amino acid appearance in individuals with UC may be indicative of amino acid depletion (Fig. 7).

9(S)-HODE and 13(R)-HODE, both oxidized lipids depicted in Fig. 8, have been found to induce the chemotaxis of monocytes in vitro [36]. The pro-inflammatory effects of 9-(S)-HODE were observed to enhance inflammation, leading to increased production of 9-(S)-HODE and lipid peroxidation.Conversely, studies have demonstrated that 13-HODE plays an anti-inflammatory role [37,38]. The findings of elevated levels of 9(S)-HODE and reduced levels of 13(R)-HODE in individuals with UC align with previous research on inflammation. Additionally, the extraction of flavonoids from SAL appeared to be more efficacious than aspirin in this study.

The migration of endothelial progenitor cells (EPCs) in response to vascular endothelial growth factor (VEGF) and stroma-derived factor-1α (SDF-1α) was significantly reduced when 20-HEDE, an antagonist of 20-HETE, was administered [39]. Further investigation is warranted to determine if 11(S)-HEDE (Fig. 8) exhibits similar functionality to 20-HEDE. Phospholipase activity during seed germination favored palmitoyl-PC and linoleoyl-PC as substrates [40]. It is of interest to explore whether 1-Palmitoyl-2-linoleoyl PE (Fig. 8) plays a comparable role.

The Musashi proteins (MSI), known as stem cell translation regulators, were found to have a significant impact on the development of the brain, blood, and epithelium [41]. This group of proteins consists of two members, namely MSI1 and MSI2. MSI2, which shares 69 % homology with MSI1, is a protein that binds to RNA molecules [42]. It was observed that MSI2 was highly expressed in myeloid leukemia cells, and its depletion resulted in reduced proliferation and increased apoptosis [43]. Interestingly, the specific inhibition of MSI2 was achieved by eicosenoic acid, a monounsaturated fatty acid [41].

The concentration of 14(Z)-Eicosenoic Acid (Fig. 8) was found to be significantly increased in individuals with ulcerative colitis (UC), but this elevation could be effectively reversed through the extraction of flavonoids from SAL. *Cis*-9,12-octadecadienoic acid (linoleic acid; LA), a polyunsaturated fatty acid (PUFA) depicted in Fig. 8, is considered crucial for human health [44]. Polyunsaturated fatty acids are essential for maintaining cell viability [45]. Dietary studies have shown that the presence of n-3 PUFAs, which are commonly found in fish oil, may lower the risk of colon cancer [46,47]. In general, the term "n-3 PUFA" refers to molecules with the first double bond located three carbon atoms away from the methyl end.

Eicosapentaenoic acid (20:5Δ5,8,11,14,17) and docosahexaenoic acid (22:6Δ4,7,10,13,16,19) were representative examples of n-3 polyunsaturated fatty acids (PUFAs) (Fig. 8). Conversely, n-6 PUFAs, such as linoleic acid (18:2Δ9,12) (Fig. 8) and arachidonic acid (20:4Δ5,8,11,14) (Fig. 6), which are commonly found in vegetable oils, were found to promote the development of colon tumors [46,48]. Furthermore, these effects were observed during both the initiation and post-initiation stages of carcinogenesis [46,49].

Among the substrates for Acyl-CoA Synthetase 5 (ACOS5), 16-hydroxyhexadecanoic acid (16OH–C16) (Fig. 9A) demonstrated the highest efficacy [50].

The clinical activity of patients diagnosed with adult-onset still's disease exhibited a significant correlation with (R)-3-hydroxyhexadecanoic acid (3OH–C16,16OH–C16 analog) [51].

Hexadecanoic acid demonstrated a strong anti-inflammatory effect [52]. Calcitriol (Fig. 9A) indirectly exerted an

anti-inflammatory effect by upregulating the anti-inflammatory cytokine IL-10 [53]. Additionally, Calcitriol inhibited the growth of colorectal cancer cell. Kirenol (Fig. 9A) was attributed with anti-inflammatory properties [54,55] Furthermore, derivatives of isosteviol (Fig. 9A) also exhibited anti-inflammatory activity [56].

Pipecolic acid levels in blood and urine were found to be associated with ataxia through peroxisomal biogenesis disorders (Fig. 9B) [57]. Lumichrome, the breakdown product of riboflavin (Fig. 9B), was observed to participate in symbiosis, leading to the reconfiguration of the host primary carbon and phytohormone metabolism, as well as hyphae initiation [58]. Lanceolatin B, one of several isolated flavonoids (Fig. 9B), exhibited anti-inflammatory properties [59]. Additionally, 4-ethylbenzoic acid (Fig. 9B) was identified as a phenolic acid in colon fermentation [60].

Apigenin, an antiproliferative flavonoid (Fig. 9B), was discovered to have inhibitory effects on tumor growth and pro-angiogenic activity [61,62]. The brown pigment present in feces was metabolized by intestinal bacteria, resulting in the production of stercobilin (Fig. 9B), which exhibited proinflammatory properties [63]. A study has reported that N-acetyl-*l*-mannosamine is a substrate with low affinity for E. coli sialic acid aldolase [64]. Additionally, N-acetyl mannosamine (Fig. 9B) has been identified as an intermediate in the biosynthesis of sialic acid [65]. Coumaric acid (Fig. 9B), a phenolic compound found in plants, was observed to either inhibit or induce the growth of the phytopathogen D. dadantii 3937 [66,67].

4.2. Key metabolic pathways

The alterations observed in the metabolites of the arachidonic acid, amino acids, and fatty acid pathways have demonstrated the significant therapeutic potential of FE within these aforementioned pathways. This study further demonstrated that the total flavonoids extracted from Sonchus arvensis L. contrast with Aspirin treatment significantly influenced 11 pathways, namely Aminoacyl-tRNA biosynthesis, Valine, leucine and isoleucine biosynthesis, Linoleic acid metabolism, PPAR signaling pathway, mTOR signaling pathway, Valine, leucine and isoleucine degradation, Lysine degradation, VEGF signaling pathway, Melanogenesis, Endocrine and other factor-regulated calcium reabsorption, and Cocaine addiction, which were associated with ulcerative colitis. The enrichment scores of the aminoacyl–tRNA biosynthesis pathway were highest, suggesting its involvement in the occurrence and/or progression of UC.

Aminoacyl-tRNA (aa-tRNA) is produced when amino acids are attached to tRNA, and it serves various biological functions [68]. The incorporation of amino acids into proteins is facilitated by aminoacyl tRNA synthetases (AARSs) [69]. The incorporation of amino acids into proteins is facilitated by aminoacyl tRNA synthetases (AARSs) [70]. Valine, leucine, and isoleucine are essential amino acids for mammals and belong to the category of branched-chain amino acids (BCAAs) [71]. Certain flavonoids have the potential to improve nonalcoholic fatty liver disease (NAFLD) in rats by modulating the metabolism pathway of alpha-linolenic acid, linoleic acid, and arachidonic acid [72]. The regulation of inflammatory responses is mediated by the PPAR nuclear receptor family [72]. The AKT/mTOR signaling pathway plays a pivotal role in governing cell proliferation, survival, and metabolism [73]. Additionally, the mTOR pathway serves as a central signaling pathway in cells, controlling multi-level gene expression [74]. Vascular endothelial growth factor (VEGF) signaling is integral to the proper functioning of blood vessels [75]. Flavonoids have the potential to induce angiogenesis in brain microvascular endothelial cells (BMECs) by activating the HIF-1α-VEGF-Notch 1 signaling pathway [76].

The presence of an excessive amount of free radicals and reactive oxygen species (ROS) has been linked to inflammatory signaling pathways [77]. One of the most significant features of UC is the increase intestinal permeability that has been linked to the pathogenesis via immune system cells [78]. Conversely, the process of melanogenesis can be hindered by both ROS generators and ROS scavengers [79]. The flavonoids of SAL may adjuncive therapy in other chronic immune-related diseases characterized by chronic inflammation such as celiac disease. Consequently, a comprehensive examination is warranted to ascertain the metabolic pathways that contribute to the development of UC and are implicated in its treatment.

4.3. Limitations

The study is subject to certain limitations, namely the utilization of a relatively small number of samples consisting of healthy C57BL/6 mice (n = 5), mice with UC (n = 5), mice treated with aspirin (n = 5), and mice treated with the total flavonoids extracted by Sonchus arvensis L. (n = 5) for the purpose of screening key metabolites. However, it adheres to the necessary criteria for animal metabolomic analysis. In order to validate the results, future research should encompass independent, large-scale studies. The findings of this study contribute to a more comprehensive comprehension of the progression of UC and offer a potential treatment approach.

5. Conclusion

A total of 73 metabolites and 14 pathways were identified via metabolomic analysis and were significantly associated with the treatment of UC. The extraction of flavonoids from SAL for the treatment of UC yields four distinct and noteworthy metabolites that exhibit characteristics differing from those of aspirin. Except for 13,14-Dihydro-15-keto-PGE2 (Fig. 6), the metabolites of Prostaglandin I2 (PGI2) (Fig. 6), (20R,22R)-20,22-dihydroxycholesterol (Fig. 9A), and PS(18:1(9Z)/0:0) (Fig. 9A) suggest that FE will induce less severe effects compared to AN. These metabolites and pathways may play a significant role in the development of UC. These findings enhance the understanding of molecular processes underlying UC and may provide potential clues for the treatment UC.

Ethics declaration statement

All experimental protocols for all animal experiments were approved by the ethics committee of Daqing Campus of Harbin Medical University (LLDQXQ2022031).

Data availability statement

The data that support the findings of this paper are available from: https://www.scidb.cn/anonymous/cmV5bWVl.

CRediT authorship contribution statement

Naidan Chang: Writing – original draft, Data curation. **Wei wei:** Methodology, Formal analysis. **Shihe Wang:** Visualization, Software, Data curation. **Shenghua Hou:** Data curation. **Yilei Sui:** Formal analysis, Data curation. **Taoyang:** Formal analysis, Data curation. **Jing He:** Formal analysis, Data curation. **Yachao Ren:** Writing – review & editing, Project administration, Funding acquisition, Conceptualization. **Guoyou Chen:** Writing – original draft, Funding acquisition, Conceptualization. **Chunlei Bu:** Project administration, Conceptualization.

Declaration of competing interest

The authors declare that they have no known competing financial interests or personal relationships that could have appeared to influence the work reported in this paper.

Acknowledgements

This work was supported by National Natural Science Foundation of China (81703426), Natural Science Foundation of Hei Long Jiang province in China (LH2023H020) and the Fundamental Research Funds for the Provincial Universities of Hei Long Jiang province (No. JFJC202202).

Appendix A. Supplementary data

Supplementary data to this article can be found online at https://doi.org/10.1016/j.heliyon.2024.e32790.

References

[1] C. Xu, W. Dong, Role of hypoxia-inducible factor-1α in pathogenesis and disease evaluation of ulcerative colitis, Exp. Ther. Med. 11 (4) (2016) 1330–1334.
[2] A. Diamanti, et al., Thalidomide as rescue therapy for acute severe ulcerative colitis, Eur. Rev. Med. Pharmacol. Sci. 18 (12) (2014) 1690–1693.
[3] D. Hu, et al., Association of ulcerative colitis with TNF-related apoptosis inducing ligand (TRAIL) gene polymorphisms and plasma soluble TRAIL levels in Chinese Han population, Eur. Rev. Med. Pharmacol. Sci. 19 (3) (2015) 467–476.
[4] P. Hoffmann, et al., Performance of tacrolimus in hospitalized patients with steroid-refractory acute severe ulcerative colitis, World J. Gastroenterol. 25 (13) (2019) 1603–1617.
[5] S.C. Ng, et al., Worldwide incidence and prevalence of inflammatory bowel disease in the 21st century: a systematic review of population-based studies, Lancet 390 (10114) (2017) 2769–2778.
[6] X. Wang, et al., Costus root granules improve ulcerative colitis through regulation of TGF-β mediation of the PI3K/AKT signaling pathway, Exp. Ther. Med. 15 (5) (2018) 4477–4484.
[7] İ.K. Önal, et al., The value of fecal calprotectin as a marker of intestinal inflammation in patients with ulcerative colitis, Turk. J. Gastroenterol. 23 (5) (2012) 509–514.
[8] L.Q. Liu, et al., Tea polysaccharide prevents colitis-associated carcinogenesis in mice by inhibiting the proliferation and invasion of tumor cells, Int. J. Mol. Sci. 19 (2) (2018).
[9] T.M. Nowacki, et al., The risk of colorectal cancer in patients with ulcerative colitis, Dig. Dis. Sci. 60 (2) (2015) 492–501.
[10] A. Granito, et al., Anti-Saccharomyces cerevisiae and perinuclear anti-neutrophil cytoplasmic antibodies in coeliac disease before and after gluten-free diet, Aliment. Pharmacol. Ther. 21 (7) (2005) 881–887.
[11] A. Granito, et al., Anti-saccharomyces cerevisiae antibodies (ASCA) in coeliac disease, Gut 55 (2) (2006) 296.
[12] Q. Li, et al., The anti-inflammatory effect of Sonchus oleraceus aqueous extract on lipopolysaccharide stimulated RAW 264.7 cells and mice, Pharm. Biol. 55 (1) (2017) 799–809.
[13] A. McDowell, et al., Antioxidant activity of puha (Sonchus oleraceus L.) as assessed by the cellular antioxidant activity (CAA) assay, Phytother Res. 25 (12) (2011) 1876–1882.
[14] D.Z. Xia, et al., Antioxidant and antibacterial activity of six edible wild plants (Sonchus spp.) in China, Nat. Prod. Res. 25 (20) (2011) 1893–1901.
[15] Y.F. Han, et al., New sesquiterpenes from Sonchus transcaspicus, Planta Med. 71 (6) (2005) 543–547.
[16] F.C. Vilela, et al., Anti-inflammatory and antipyretic effects of Sonchus oleraceus in rats, J. Ethnopharmacol. 127 (3) (2010) 737–741.
[17] K. Bisht, K.H. Wagner, A.C. Bulmer, Curcumin, resveratrol and flavonoids as anti-inflammatory, cyto- and DNA-protective dietary compounds, Toxicology 278 (1) (2010) 88–100.
[18] P. Singh, A. Anand, V. Kumar, Recent developments in biological activities of chalcones: a mini review, Eur. J. Med. Chem. 85 (2014) 758–777.
[19] J. Xia, D.S. Wishart, MSEA: a web-based tool to identify biologically meaningful patterns in quantitative metabolomic data, Nucleic Acids Res. 38 (Web Server issue) (2010) W71–W77.
[20] K. Hollywood, D.R. Brison, R. Goodacre, Metabolomics: current technologies and future trends, Proteomics 6 (17) (2006) 4716–4723.
[21] C.H. Johnson, et al., Xenobiotic metabolomics: major impact on the metabolome, Annu. Rev. Pharmacol. Toxicol. 52 (2012) 37–56.

[22] T. Matsubara, et al., Metabolomics identifies an inflammatory cascade involved in dioxin- and diet-induced steatohepatitis, Cell Metabol. 16 (5) (2012) 634–644.
[23] X. Zhao, et al., Serum metabolomics study of polycystic ovary syndrome based on liquid chromatography-mass spectrometry, J. Proteome Res. 13 (2) (2014) 1101–1111.
[24] T. Altadill, et al., Enabling metabolomics based biomarker discovery studies using molecular phenotyping of exosome-like vesicles, PLoS One 11 (3) (2016) e0151339.
[25] D. Schultz, et al., Eicosanoid profile of influenza A virus infected pigs, Metabolites 9 (7) (2019).
[26] K.E. Olagaray, et al., Postpartum meloxicam administration alters plasma haptoglobin, polyunsaturated fatty acid, and oxylipid concentrations in postpartum ewes, J. Anim. Sci. Biotechnol. 11 (2020) 68.
[27] C.M. Davis, et al., Ultrasound stimulates formation and release of vasoactive compounds in brain endothelial cells, Am. J. Physiol. Heart Circ. Physiol. 309 (4) (2015) H583–H591.
[28] L. Wu, et al., PPARα ligand, AVE8134, and cyclooxygenase inhibitor therapy synergistically suppress lung cancer growth and metastasis, BMC Cancer 19 (1) (2019) 1166.
[29] E. Cecerska-Heryć, et al., Effect of renal replacement therapy on selected arachidonic acid derivatives concentration, BMC Nephrol. 21 (1) (2020) 394.
[30] B.C. Jiang, et al., Notch signaling regulates circulating T helper 22 cells in patients with chronic hepatitis C, Viral Immunol. 30 (7) (2017) 522–532.
[31] X. Wei, et al., Notch signaling contributes to liver inflammation by regulation of interleukin-22-producing cells in hepatitis B virus infection, Front. Cell. Infect. Microbiol. 6 (2016) 132.
[32] Y. Li, et al., Exogenous stimuli maintain intraepithelial lymphocytes via aryl hydrocarbon receptor activation, Cell 147 (3) (2011) 629–640.
[33] I. Aronchik, et al., The antiproliferative response of indole-3-carbinol in human melanoma cells is triggered by an interaction with NEDD4-1 and disruption of wild-type PTEN degradation, Mol. Cancer Res. 12 (11) (2014) 1621–1634.
[34] M. Lappalainen, et al., Novel biomarker candidates for febrile neutropenia in hematological patients using nontargeted metabolomics, Dis. Markers 2018 (2018) 6964529.
[35] P. Banerjee, V.A.O. Carmelo, H.N. Kadarmideen, Integrative analysis of metabolomic and transcriptomic profiles uncovers biological pathways of feed efficiency in pigs, Metabolites 10 (7) (2020).
[36] J. Rolin, Z. Al-Jaderi, A.A. Maghazachi, Oxidized lipids and lysophosphatidylcholine induce the chemotaxis and intracellular calcium influx in natural killer cells, Immunobiology 218 (6) (2013) 875–883.
[37] V. Vangaveti, B.T. Baune, R.L. Kennedy, Hydroxyoctadecadienoic acids: novel regulators of macrophage differentiation and atherogenesis, Ther Adv Endocrinol Metab 1 (2) (2010) 51–60.
[38] R. Altmann, et al., 13-Oxo-ODE is an endogenous ligand for PPARgamma in human colonic epithelial cells, Biochem. Pharmacol. 74 (4) (2007) 612–622.
[39] A.M. Guo, et al., The cytochrome P450 4A/F-20-hydroxyeicosatetraenoic acid system: a regulator of endothelial precursor cells derived from human umbilical cord blood, J Pharmacol Exp Ther 338 (2) (2011) 421–429.
[40] C. May, et al., A phospholipase A2 is transiently synthesized during seed germination and localized to lipid bodies, Biochim. Biophys. Acta 1393 (2–3) (1998) 267–276.
[41] C.C. Clingman, et al., Allosteric inhibition of a stem cell RNA-binding protein by an intermediary metabolite, Elife 3 (2014).
[42] S. Sakakibara, et al., RNA-binding protein Musashi family: roles for CNS stem cells and a subpopulation of ependymal cells revealed by targeted disruption and antisense ablation, Proc Natl Acad Sci U S A 99 (23) (2002) 15194–15199.
[43] M.G. Kharas, et al., Musashi-2 regulates normal hematopoiesis and promotes aggressive myeloid leukemia, Nat Med 16 (8) (2010) 903–908.
[44] K.R. Lee, et al., High accumulation of γ-linolenic acid and Stearidonic acid in transgenic Perilla (Perilla frutescens var. frutescens) seeds, BMC Plant Biol. 19 (1) (2019) 120.
[45] W. Stoffel, et al., Dietary ω3-and ω6-Polyunsaturated fatty acids reconstitute fertility of Juvenile and adult Fads2-Deficient mice, Mol Metab 36 (2020) 100974.
[46] B.S. Reddy, C. Burill, J. Rigotty, Effect of diets high in omega-3 and omega-6 fatty acids on initiation and postinitiation stages of colon carcinogenesis, Cancer Res. 51 (2) (1991) 487–491.
[47] G.K. Pot, et al., Opposing associations of serum n-3 and n-6 polyunsaturated fatty acids with colorectal adenoma risk: an endoscopy-based case-control study, Int. J. Cancer 123 (8) (2008) 1974–1977.
[48] J. Whelan, M.F. McEntee, Dietary (n-6) PUFA and intestinal tumorigenesis, J. Nutr. 134 (12 Suppl) (2004) 3421S–3426S.
[49] W.C. Chang, R.S. Chapkin, J.R. Lupton, Predictive value of proliferation, differentiation and apoptosis as intermediate markers for colon tumorigenesis, Carcinogenesis 18 (4) (1997) 721–730.
[50] C. de Azevedo Souza, et al., A novel fatty Acyl-CoA Synthetase is required for pollen development and sporopollenin biosynthesis in Arabidopsis, Plant Cell 21 (2) (2009) 507–525.
[51] D.Y. Chen, et al., Metabolic disturbances in adult-onset still's disease evaluated using liquid chromatography/mass spectrometry-based metabolomic analysis, PLoS One 11 (12) (2016) e0168147.
[52] O. Olorundare, et al., Irvingia gabonensis seed extract: an effective attenuator of doxorubicin-mediated cardiotoxicity in wistar rats, Oxid. Med. Cell. Longev. 2020 (2020) 1602816.
[53] E. Maquigussa, et al., Calcitriol ameliorates renal damage in a pre-established proteinuria model, Mol. Med. Rep. 12 (1) (2015) 1009–1015.
[54] T.D. Nguyen, et al., Anti-hyperuricemic, anti-inflammatory and analgesic effects of siegesbeckia orientalis L. Resulting from the fraction with high phenolic content, BMC Complement Altern Med 17 (1) (2017) 191.
[55] J.P. Wang, et al., Topical anti-inflammatory and analgesic activity of kirenol isolated from Siegesbeckia orientalis, J. Ethnopharmacol. 137 (3) (2011) 1089–1094.
[56] S.F. Chang, et al., Microbial transformation of isosteviol and bioactivities against the glucocorticoid/androgen response elements, J Nat Prod 71 (1) (2008) 87–92.
[57] S.J. Steinberg, et al., Peroxisome biogenesis disorders, Biochim. Biophys. Acta 1763 (12) (2006) 1733–1748.
[58] L.M. Gouws, et al., The plant growth promoting substance, lumichrome, mimics starch, and ethylene-associated symbiotic responses in lotus and tomato roots, Front. Plant Sci. 3 (2012) 120.
[59] X. Huo, et al., Antiinflammatory and analgesic activities of ethanol extract and isolated compounds from Millettia pulchra, Biol. Pharm. Bull. 38 (9) (2015) 1328–1336.
[60] L. Zhu, et al., The composition and antioxidant activity of bound phenolics in three legumes, and their metabolism and bioaccessibility of gastrointestinal tract, Foods 9 (12) (2020).
[61] W. Wu, et al., Preparation, characterization and antitumor activity evaluation of apigenin nanoparticles by the liquid antisolvent precipitation technique, Drug Deliv. 24 (1) (2017) 1713–1720.
[62] Y. Xiang, et al., Houshiheisan promotes angiogenesis via HIF-1α/VEGF and SDF-1/CXCR4 pathways: in vivo and in vitro, Biosci. Rep. 39 (10) (2019).
[63] S. Sanada, et al., Intestinal microbial metabolite stercobilin involvement in the chronic inflammation of ob/ob mice, Sci. Rep. 10 (1) (2020) 6479.
[64] C.C. Hsu, et al., Directed evolution of D-sialic acid aldolase to L-3-deoxy-manno-2-octulosonic acid (L-KDO) aldolase, Proc Natl Acad Sci U S A 102 (26) (2005) 9122–9126.
[65] F. Monaco, J. Robbins, Incorporation of N-acetylmannosamine and N-acetylglucosamine into thyroglobulin in rat thyroid in vitro, J. Biol. Chem. 248 (6) (1973) 2072–2077.
[66] S. Yang, et al., Type III secretion system genes of Dickeya dadantii 3937 are induced by plant phenolic acids, PLoS One 3 (8) (2008) e2973.
[67] Y. Li, et al., The plant phenolic compound p-coumaric acid represses gene expression in the Dickeya dadantii type III secretion system, Appl. Environ. Microbiol. 75 (5) (2009) 1223–1228.
[68] H. Gamper, Y.M. Hou, tRNA 3'-amino-tailing for stable amino acid attachment, RNA 24 (12) (2018) 1878–1885.

[69] C.W. Carter Jr., Cognition, mechanism, and evolutionary relationships in aminoacyl-tRNA synthetases, Annu. Rev. Biochem. 62 (1993) 715–748.
[70] M. Zhou, et al., Crystal structures of Saccharomyces cerevisiae tryptophanyl-tRNA synthetase: new insights into the mechanism of tryptophan activation and implications for anti-fungal drug design, Nucleic Acids Res. 38 (10) (2010) 3399–3413.
[71] M. Zhou, et al., Targeting BCAA catabolism to treat obesity-associated insulin resistance, Diabetes 68 (9) (2019) 1730–1746.
[72] H. Cui, et al., Untargeted metabolomic analysis of the effects and mechanism of nuciferine treatment on rats with nonalcoholic fatty liver disease, Front. Pharmacol. 11 (2020) 858.
[73] W. Wang, et al., MAPK4 promotes triple negative breast cancer growth and reduces tumor sensitivity to PI3K blockade, Nat. Commun. 13 (1) (2022) 245.
[74] M. Schüle, et al., mTOR driven gene transcription is required for cholesterol production in neurons of the developing cerebral cortex, Int. J. Mol. Sci. 22 (11) (2021).
[75] Y. Takeda, et al., Diminished metastasis in tetraspanin CD151-knockout mice, Blood 118 (2) (2011) 464–472.
[76] Q.S. He, et al., Protective effects of total flavonoids in Caragana against hypoxia/reoxygenation-induced injury in human brain microvascular endothelial cells, Biomed. Pharmacother. 89 (2017) 316–322.
[77] Y.S. Ho, J.Y. Wu, C.Y. Chang, A new natural antioxidant biomaterial from cinnamomum osmophloeum kanehira leaves represses melanogenesis and protects against DNA damage, Antioxidants 8 (10) (2019).
[78] L. Aldars-García, et al., The interplay between immune system and microbiota in inflammatory bowel disease: a narrative review, Int. J. Mol. Sci. 22 (6) (2021).
[79] H. Yasui, H. Sakurai, Age-dependent generation of reactive oxygen species in the skin of live hairless rats exposed to UVA light, Exp. Dermatol. 12 (5) (2003) 655–661.